

1N-18
209764
32 p

Structural Evaluation of Concepts for a Solar Energy Concentrator for Space Station Advanced Development Program

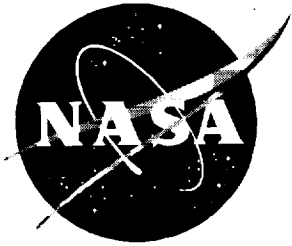
Winfred S. Kenner and Marvin D. Rhodes

(NASA-TP-3375) STRUCTURAL
EVALUATION OF CONCEPTS FOR A SOLAR
ENERGY CONCENTRATOR FOR SPACE
STATION ADVANCED DEVELOPMENT
PROGRAM (NASA) 32 p

N94-26609

Unclass

H1/18 0209764



Structural Evaluation of Concepts for a Solar Energy Concentrator for Space Station Advanced Development Program

*Winfred S. Kenner and Marvin D. Rhodes
Langley Research Center • Hampton, Virginia*

Abstract

Solar dynamic power systems have a higher thermodynamic efficiency than conventional photovoltaic systems; therefore, they are attractive for long-term space missions with high electrical power demands. In an investigation conducted in support of a preliminary concept for Space Station Freedom, a novel approach for a solar dynamic power system was developed and a number of the components for the solar concentrator were fabricated for experimental evaluation. The concentrator consists of hexagonal panels made up of triangular reflective facets which are supported by a truss. In the current investigation, structural analyses of the solar concentrator and the support truss were conducted using finite-element models. As a part of the investigation, a number of potential component failure scenarios were postulated and the resulting structural performance was assessed. The solar concentrator and support truss were found to be adequate to meet a 1.0-Hz structural dynamics design requirement in pristine condition. However, for some of the simulated component failure conditions, the fundamental frequency dropped below the 1.0-Hz design requirement. As a result, two alternative concepts were developed and assessed. One concept incorporated a tetrahedral ring truss support for the hexagonal panels; the second incorporated a full tetrahedral truss support for the panels. The results indicate that significant improvements in stiffness can be obtained by attaching the panels to a tetrahedral truss, and that this concentrator and support truss will meet the 1.0-Hz design requirement with any of the simulated failure conditions.

Introduction

The development and use of solar dynamic systems to supply power for space missions has been a goal of NASA for many years (ref. 1). Solar dynamic systems have a relatively high thermodynamic operating efficiency compared with photovoltaic systems; therefore, they are particularly attractive for long-term missions with high electrical power demands. An application for these systems is an astronaut-tended space station, illustrated in figure 1. An astronaut-tended space station is a large complex spacecraft requiring assembly in orbit. In an investigation conducted in support of a preliminary concept for Space Station Freedom, a novel approach for a solar dynamic power system was developed. A number of the components for the system, known as a solar concentrator, were fabricated for evaluation (ref. 2). This concentrator concept consists of 19 flat hexagonal truss panels, arranged to best fit a parabolic contour, and an offset heat receiver. Each panel has 24 spherically contoured reflective facets. The initial evaluation (ref. 2) consisted of an optical performance ray-trace test, a cursory assessment of the truss panel assembly operations, and a limited finite-element structural dynamics analysis. This evaluation did not consider potential structural

component failure conditions, and the assembly procedure apparently did not address how components that degraded or failed during service would be replaced. Component failure and replacement during long-term missions can affect operational conditions, stability and control, and astronaut safety during the repair process. A postflight inspection of a recent Space Shuttle mission (STS-45), data on space debris (ref. 3), and inspection of the Long Duration Exposure Facility (LDEF) satellite all indicate that the potential for performance-degrading structural impacts is of serious concern.

The purpose of the investigation described herein was to expand the structural assessment of the concentrator assembly and its support system. The present investigation included a detailed review of the proposed on-orbit assembly procedures and an expanded finite-element structural analysis of the initial design concept. As a part of the current study, a number of potential component failure scenarios were postulated, and the resulting structural performance was assessed. Conditions required to initiate the proposed failures were not experimentally simulated, and specific requirements to initiate the failure were not postulated; the failed component was simply removed from the model. In a flight mission, local

response with the failed component in place would have to be analyzed when developing repair procedures, because the failed component may affect astronaut safety. Those component failures that degraded structural performance significantly were examined to identify improvements and alternative structural concepts that might be incorporated in the structural design of the solar concentrator. In this paper, the initial design concept as it was detailed in references 2, 4, and 5 is presented, and two alternative structural concepts developed during the current investigation, along with the supporting finite-element analysis, are discussed.

System Description

The novel solar dynamic module proposed for Space Station *Freedom* and evaluated in the current study is shown mounted to a truss beam in figure 2. Also identified in the figure are some of the various system components and their relative locations in the assembled system. The solar dynamic module is designed to provide approximately 25 kW of electrical power and to operate with minimal service for a 25- to 30-year period. The module is mounted on a rotary joint (called a beta gimbal) that is attached to the truss beam. The radiator assembly (for heat rejection) is positioned normal to the concave surface of the reflector assembly to minimize shading of the concentrator. The reflector assembly and support structure are attached to a mounting plate (pointing gimbal) near the heat receiver/converter. This mounting plate is part of the fine pointing control and is positioned by two actuators (not shown) that are located in the interface structural assembly. Additional details of the overall design can be found in reference 4.

The assembly sequence proposed by the initial development team is illustrated in figure 3. The system is designed to be mounted on a pallet for launch into orbit on a single Space Shuttle flight. In orbit, the pallet would be transferred to a mobile transporter and moved to the operational site for assembly by two attending astronauts assisted by a long, robotically operated boom (fig. 3(a)). At the assembly site, the beta gimbal and interface truss are assembled, and then the radiator and the heat receiver/converter are installed. The solar concentrator support structure (fig. 3(b)) consists of nine tubular members. Three of the members span the concentrator and are attached to it at points on the periphery to form a triangle that is called the delta truss; the remaining six supporting members secure the solar concentrator to the mounting plate. Astronauts initiate the assembly of the solar concentrator panels by latching the center

panel to a grapple fixture on the robot boom. They continue assembly by removing panels from the storage pallet and pushing them into position (fig. 3(c)), where the panels are automatically latched together by spring-actuated connectors. The boom rotates the assembled panels into the proper orientation and is moved away from the pallet as each panel ring is completed. The panel assembly latching sequence is shown in figure 3(d). The panel insertion sequence is novel because each panel can be inserted directly from the storage canister by two strategically positioned astronauts. After all 19 panels have been installed to complete the concentrator, the robot boom positions the concentrator for attachment to the support truss (fig. 3(e)). Three spring-loaded latches automatically capture the concentrator to secure it to the support truss. One of the principal design requirements (ref. 5) was that the assembled concentrator have adequate stiffness so that the fundamental frequency is greater than 1.0 Hz. This requirement keeps component structural frequencies outside the bandwidth of the space station control frequencies. Additional information on both the concept and the hardware is discussed in following sections.

Concentrator Models

The focus points of the current study were the structural behavior of the solar concentrator assembly and the structural support truss. During this investigation, three structural concepts for the concentrator were evaluated. The original, or baseline concept developed by the initial design team, referred to hereinafter as concept A, was evaluated first. Modifications to both the concentrator and the support structure were developed to address problems that became apparent as the study progressed. These modifications produced concepts B and C.

Concept A

The baseline concentrator configuration is shown in figure 4. This configuration consists of the 19 panels that compose the reflector assembly and the 9 members that compose the support structure. The support structure contains three delta truss members that span the concave face of the reflector and are attached to the reflector at the periphery. The support structure also contains truss members that attach the reflector panel assembly to the mounting plate. The views of the concentrator on the left of figure 4 indicate the plane of symmetry of the panels and the position of the support truss members; the heat receiver and power module are positioned to the left of the concentrator centerline but are not shown in the figure. The symmetry axis is a mirror

plane of symmetry for the concentrator panels, the delta truss, and the support truss; the heat receiver is offset from the concentrator centerline to minimize blockage of incident rays. Because of the symmetry, the two middle delta members have a common length; the rear delta member is moderately shorter. The offset of the centerline and the symmetry plane cause the support truss members to have different lengths. Those support members identified in the figure by the same names (rear, middle, and front support members) are of equal lengths.

Details of the hexagonal panels of the concentrator, the panel latches, and the installation sequence are shown in figure 5. The concentrator assembly consists of 19 hexagonal panels connected by 60 latches. The locations of the latches are indicated by the line segments between the panels in figure 5(a). The panels are flat open-grid structures that are subdivided into six large equilateral triangles. The structural members of the panels include six radial members and six perimeter members. All these members are box-beam sections that are fabricated from graphite-epoxy and bonded to metallic corner fittings. Each of the large triangles is subdivided into four smaller equilateral triangles that represent reflective facets as noted in figure 5(b). The desired parabolic contour of the concentrator is approximated by the selective use of spherically contoured facets. For the 456 reflective facets required to fully populate the 19 panels, 4 different radii of curvature are used. The facets are constructed with graphite-epoxy face sheets bonded to a honeycomb core. A vapor-deposited metallic surface with a protective overcoating is used to form the reflective surface. The facets are designed to be self-supporting and to withstand launch loads, but not to provide structural support to the hexagonal panels. The facets are attached to the graphite-epoxy box beams by aluminum standoff rods at each of the apexes of the facet. Details of the facets can be found in reference 5.

The flat hexagonal panels are attached to form a faceted shell-type structure that is approximately 54.8 ft in diameter. The panels are moved radially toward the center during installation and are held together by latches (fig. 5). The latches are located near the apexes of the panels to minimize bending loads in the box-beam perimeter members. A typical latch mechanism that connects the front of panel 19 to the rear of panel 7 is shown in figure 5(c). The receptacle portion is mounted to the panel that has been previously installed (panel 7), and the insertion mechanism is mounted to the panel that is being installed (panel 19). The receptacle has a socket

with a spring-loaded pawl that admits a metallic sphere, which is mounted to the insertion mechanism. After the sphere is inserted into the receptacle, the front face of the pawl restrains the sphere and holds the panel in place. The latches individually provide axial and lateral force restraint but do not provide rotational restraint.

The locations of the latches and the assembly require that four different latch types be used. Each latch type employs the same ball-and-receptacle configuration illustrated in figure 5; however, the insertion direction is different for each of the four types. The different insertion directions are necessary to permit the panel sides to be latched (note side latches on panel 19 of fig. 5(a)) when the panel is inserted in a radial direction. Removal of a panel for repair or replacement requires simultaneous release of all latches. To accomplish this task, the latch pawl must be manually retracted by overriding the spring force and any accumulated wedging forces. Also, to repair or replace panels in either of the interior rings, at least three other panels have to be removed and stored to provide access.

Each of the hexagonal panels is about 13.5 ft wide from apex to apex through the panel center (11.8 ft wide from side to side), and 4.5 in. thick. The total mass of the concentrator assembly and the nine-member structural support truss is estimated to be 1975.4 lb (ref. 4). The mass is apportioned as follows: panel frames, 636.5 lb; facets and supporting hardware, 912.0 lb; panel latches, 252.0 lb; delta truss, 67.5 lb; and support truss, 107.4 lb. Additional details of the concept, including fabrication of the hardware components, can be found in reference 5.

Concept B

A schematic of concept B is shown in figure 6. Concept B includes the same concentrator panel assembly and latch system described previously for concept A. However, the three-member delta truss of the concept A concentrator is replaced by a multi-member tetrahedral ring truss attached to the back of the concept B panel assembly. In addition, three support members have been added to the support truss, one at each concentrator support point. The ring truss consists of 132 members. The ring truss, because of its redundancy, makes the concept B concentrator less susceptible to structural degradation than the concept A concentrator in the event of failure of a single member. To match the contour of the reflector assembly, the ring truss members vary slightly in length, averaging about 140 in. The material and geometric properties of the truss members were obtained from studies of large segmented

reflectors reported in reference 6, and are discussed in the "Finite-Element Models" section.

The panels for concept B may be assembled in the same manner and sequence as for concept A, and the perimeter truss can be assembled strut by strut before the concentrator is attached to the support truss. Assembly techniques for trusses of this type have been developed and experimentally verified in neutral buoyancy tests (ref. 7). In addition to the panels being latched together as described previously, the truss is attached at three locations to each of the outer perimeter panels. A sketch of the truss-to-panel attachment configuration is shown in figure 7. Three panels are identified in the figure to highlight details of the configuration. The geometry of the truss is shown, including the surfaces on which the nodes are located with respect to the reflector panels. The truss nodes adjacent to the panels are indicated by filled circles and are identified as the top-surface nodes. The nodes indicated by open circles lie on the opposite surface and are identified as bottom-surface nodes. The terms "top" and "bottom" do not necessarily relate to vertical positions but are used herein to distinguish between surfaces. The truss members on the top and bottom surfaces are indicated by solid lines; the members connecting nodes on these two surfaces, referred to as core members, are denoted by dashed lines. To connect the panels and ring truss together, a truss-to-panel attachment fitting was located on the top-surface nodes of the truss. The detailed mechanical design of the truss-to-panel attachment fitting has not been defined, as the current study was focused only on conceptual development and preliminary structural analysis. The structural specifications of the attachment fitting required for parametric studies are outlined in the "Finite-Element Models" section.

Concept C

A schematic of concept C is shown in figure 8. Concept C is similar to concept B in that a multimember tetrahedral truss is attached to the rear of the concentrator. However, unlike the ring truss of concept B, the rear-mounted truss in concept C is fully populated. The full truss is composed of 162 members and 46 nodes. For this configuration, a truss section is located behind each of the 19 panels; therefore, all panel-to-panel latches are removed and each panel is considered to be attached only to the truss at three apexes. The same truss-to-panel attachment fittings illustrated in figure 7 for concept B are assumed for concept C. Also, the same nine-member support truss described for concept B is used for concept C.

Finite-Element Models

Finite-element models were developed to determine the dynamic characteristics of the three concentrator models. A representation of the finite-element model for concept A is shown in figure 9, and the mass and structural properties are listed in tables 1 and 2. The models were developed using beam elements for the component members. Experimental stiffness and mass properties for the hardware were obtained from data reported in references 4 and 5. Engineering estimates for structural properties and masses were used for those components for which detailed designs have not been developed. As indicated in figure 9, a relatively simple coarse-grid model was used to get an overall perspective of the system behavior. Nonstructural components, such as the spherical reflector facets, were included as nonstructural mass at appropriate finite-element node locations. The models were developed for use by the finite-element computer program Engineering Analysis Language (EAL) described in reference 8.

The latches (fig. 5(c)) were modeled with beam-type finite elements as indicated in figure 9. The stiffness characteristics of the latch type shown in figure 5(c) were obtained from test information supplied by researchers at Lewis Research Center. Typical load-displacement results are shown in figure 10. The latch was loaded first in compression and then cycled into tension. The wedging force of the latch increases on each load cycle because of rotation of the latch pawl. The increasing wedge force is probably responsible for the slight shift in zero-load displacement from cycle to cycle. It may also be responsible for the increase in the tension load at which the stiffness change occurs. In the finite-element model, the node between the elements of the latch was modeled as a pin connection with axial and lateral stiffness but with no resistance to axial or lateral rotation. The axial stiffness used in the finite-element model was taken from the linear portion of figure 10 at zero load and is listed in table 2. The lateral stiffness values were obtained from test data supplied by research engineers at Lewis Research Center and are listed in table 2. It was noted previously that four latch configurations were required to assemble all 19 panels. However, the stiffness results reported in figure 10 for the latch configuration illustrated in figure 5 were the only structural information available on the panel latches; therefore, for modeling purposes, all the latches were assumed to exhibit the same load-deflection response. This assumption could cause the stiffness of the system to be overestimated if the side-entry joints are not as stiff as those illustrated in figure 5. As a precaution,

calculations were performed for a range of assumed latch stiffnesses. Details of the analysis and numerical results are presented in the "Results and Discussion" section.

The rear-mounted tetrahedral trusses of concepts B and C were modeled with one beam element per member. The structural and mass properties used for these elements are also listed in tables 1 and 2. These properties were selected from studies of trusses designed to support precision segmented reflectors (ref. 6). The truss members are similar to beams that are clamped at both ends, and the fundamental natural frequency of a member was determined to be significantly higher than the fundamental natural frequency of the truss and panel system for every configuration analyzed in this study. The fittings that attach the hexagonal panels to the truss in concepts B and C were also modeled as beam elements; the properties of these elements are also listed in tables 1 and 2.

Analysis

Finite-element analyses of the three concentrator concepts were conducted, and the natural modes and frequencies of each concept were determined and compared. Also, the vibration mode shapes were examined with the aid of a computer-animation routine; as a result, component interaction and the relative levels of response of the various components within each concept could be examined. The strain energy in the various structural units (panels, truss, and support members) was computed and used as an aid in evaluating and comparing results. All three concepts were evaluated for various local failure scenarios, ranging from failure of a single latch or panel-frame member to failure of one of the struts in the delta truss and/or support truss. Component failures were simulated by removing a member and examining the resulting structural modes and frequencies. A component failure was considered to be tolerable if the resulting frequency was approximately the same as the frequency with the component intact and if the frequency was still greater than 1.0 Hz.

The support members were modeled attached to a rigid base as shown by the axonometric view in figure 9. This configuration is similar to a cantilever beam (represented by the support truss members) supporting a tip mass (represented by the concentrator panels and delta truss). Since little structural information was available on the design characteristics and stiffness of the pointing gimbal and mounting plate, all three concepts were assumed to be supported in this manner. However, the effect of this support condition was evaluated for concept A by

examining the effect of base stiffness on the structural modes and frequencies.

In addition to the analyses of the three concepts, model evaluation studies were performed to provide fundamental insight into the structural mechanics of the concepts. For example, the effect of the delta truss on the response of the concentrator panel assembly as illustrated in figure 11 was examined by analyzing the panel assembly with and without the three members of the delta truss. The free-free response of the reflector panel assembly with the ring truss (concept B) and with a full truss (concept C) was also examined. For concept A, the effect of latch stiffness on the overall response was also parametrically examined.

Results and Discussion

The mode shapes and frequencies for the first four modes of concept A are shown in figure 12. In addition, the relative strain energies in the panels, support members, and delta truss members are listed in the figure, and the component with the highest percentage of strain energy for each mode is highlighted. The first mode is above the 1.0-Hz design minimum and is about the same as that reported in reference 5. All the frequencies are in the range of 1.64 to 2.30 Hz. The first and second modes of concept A are similar to those of a cantilever beam; the combined panel assembly and delta truss represent a tip mass. The first mode is a flexural beam and the second mode is torsional. Both the mode shape and the strain energy distribution confirm this conclusion. Figure 12 also illustrates the relative displacements and the approximate locations of the node lines for modes 3 and 4, which principally involve panel assembly deformation. The "+" and "-" signs shown on the top view indicate regions of the deformation phase.

The analysis for concept A was based on the assumption that the support members are attached to a rigid base. Since the response for the first two modes of the system are similar to the first two modes of a cantilever beam, the end fixity can have a significant effect on the system behavior. Therefore, an analysis was conducted with the rear support members modeled as pinned at the base and with the middle and front support members modeled as attached to the base by linear extensional springs. This configuration is similar to a beam supported by a torsional spring at the root. The effect of the base support condition on the fundamental frequency is illustrated in figure 13. The fundamental frequency is shown in the figure as a function of the root spring

stiffness. For this analysis, the tip mass of the cantilever beam was equal to the combined mass of the concentrator and the delta truss, the length of the beam was the same as the distance from the center panel to the base, and the bending stiffness of the beam was calculated based on a fundamental frequency of 1.64 Hz (the frequency of the total system). The equivalent torsional stiffness at the base of the beam is determined by multiplying the extensional stiffness of the spring by the distance between the supports. The data shown in figure 13 indicate that the finite-element model and the classical torsional-spring-supported beam give similar results. The results indicate that for the frequency (mode 1) reported herein to be valid for a space operating system, the mounting-plate support base must have a torsional spring stiffness of at least 1×10^8 in-lb. The information on the design in references 2, 4, and 5 is insufficient for evaluation of the actual stiffness of the base mounting plate.

The free-free vibration of the reflector system with and without the delta truss was examined to quantify the stiffening effect of the delta truss on the panel assembly. The first four structural vibration frequencies and mode shapes are shown in figure 14. The frequencies for the two assemblies shown in figure 14 indicate that the delta truss significantly stiffens the reflector assembly. The frequencies and mode shapes for the first and third modes of the reflector with the delta truss (fig. 14) are similar to the third and fourth modes of concept A (fig. 12), because those modes of concept A primarily involved panel response. The slight differences in frequencies indicate the presence of the support members in concept A and the absence of support members in the free-free model.

A parametric analysis was conducted to determine the influence of the latch stiffness on the fundamental frequency of the free-free panel assembly and delta truss of concept A. The results are shown in figure 15. Although four different types of latches were used for this analysis, it was assumed that all latches had equal axial stiffness. The latch stiffness, originally obtained from the latch load-deflection plot shown in figure 10, was varied in increments of ten and the resulting frequencies and mode shapes were determined. The results shown in figure 15 indicate that the fundamental frequency of the panel assembly is relatively insensitive to changes in the latch stiffness when the latch stiffness is greater than 1×10^5 lb. Therefore, even though the latches were significantly more compliant than the box-beam sections of the panels to which they connect, the relatively low latch stiffness did not significantly reduce the fundamental

frequency of the total panel assembly. These results also indicate that the assumption of equal axial stiffness for all latches appears to have little adverse effect on the total system results.

The effect of simulated structural component failures on the fundamental frequency of concept A is shown in table 3. The failures were simulated by removing the indicated components from the finite-element model. The results shown in table 3 include only the worst condition for simulated panel latch failure. Several latch failures were evaluated; however, the frequency shown was the lowest obtained for all such failure conditions. Only those failures that involve the delta and support truss members lower the frequency below the 1.0-Hz limit; therefore, failure of the delta and support truss members defines the critical condition. These results led directly to the incorporation of the rear-mounted tetrahedral truss and to the three support members that were added to concepts B and C.

The first four calculated mode shapes, frequencies, and strain energy distributions of concept B, in which the panels are supported by a rear-mounted tetrahedral ring truss, are shown in figure 16. The first two mode shapes of concept B are nominally the same cantilever beam bending and torsion modes as those of concept A (fig. 12). The three additional truss members add enough stiffness to support the additional mass of the ring truss so that the first two frequencies are basically the same for concepts A and B. The frequencies of the third and fourth modes of concept B are approximately 50 percent higher than the corresponding frequencies for concept A. Also, they involve simple beam-type deformations of the individual support and delta truss members, whereas these modes in concept A were characterized by significant panel deformation. A comparison of the strain energy in the panels for the first 4 modes of concepts A and B shows that the panel strain energy is significantly lower in concept B than in concept A. This difference indicates that the panels and rear-mounted ring truss of concept B are significantly stiffer than the interconnected panels and delta truss of concept A. (A direct comparison of the panel configurations for all three concepts follows.) The additional mass for the rear-mounted ring truss in concept B is approximately 400 lb, or 20 percent of the baseline configuration.

Several simulated failure conditions of concept B were analyzed. The results are shown in table 4. None of the simulated failures cause the fundamental frequency to fall below the mandated 1.0-Hz minimum. The addition of the three support members (fig. 6) removes the critical support-member failure

condition noted for concept A. Failure of any single rear-mounted truss member is not likely to result in a significant decrease in frequency, because this portion of the structure is highly redundant.

The first four vibration frequencies and mode shapes of concept C, for which the reflector panels are supported by a rear-mounted full truss, are shown in figure 17. The frequencies for all three concepts are listed in table 5. The frequencies and mode shapes of concepts B and C are essentially the same and are dominated by the support members. The small differences in frequencies are caused by the 165-lb mass difference between the two configurations. The difference in mass results from the absence of the 60 panel latches and the addition of 4 truss nodes and 30 struts in concept C. The effect of simulated failure of the support members for concept C was determined to be the same as for concept B; that is, no simulated single-component failure reduced the frequency below the mandated value of 1.0 Hz.

The panel assemblies for concepts B and C without the support members were analyzed as free-free units. These configurations are illustrated in figure 18, the vibration frequencies are listed in table 6, and the mode shapes are presented in figure 19. The mode shapes shown in figure 19 for the two concepts are identical; however, the frequencies shown in table 6 are slightly different. This difference may be caused by the lower mass of concept C and by the shift in mass distribution. Concept B has more mass near the periphery than concept C because of the presence of the panel latches and the absence of the tetrahedral truss in the center. The frequencies for concepts B and C are more than four times higher than those for concept A with the delta truss. These results demonstrate that a truss provides significantly more structurally efficient support for a set of panels that approximates a shallow paraboloid than a set of interpanel latches and three tubular beam members. The results also indicate that, based on the mass and structural stiffness of these components, a full truss support is as structurally efficient as a ring truss supplemented by interpanel latches. The full truss may be easier to design, fabricate, and assemble than the ring truss and panel latches, because of the redundancy in the panel latch and truss-to-panel attachment mechanism. Although the proposed solar dynamic concentrator system is adequate to meet the design requirements, the results of this study indicate that significant improvements in stiffness can be obtained under normal conditions, and especially under conditions of structural component failure, by incorporating a support truss for the panels.

Concluding Remarks

Solar dynamic systems are attractive sources of electric power for long-term space missions because of their high thermodynamic operating efficiency. In a preliminary design study for Space Station *Freedom*, a novel concept for a solar dynamic power system was developed and a number of components for the solar concentrator were fabricated for experimental evaluation. The solar concentrator consists of 19 flat truss panels that are latched together and supported by 3 tubular members that span the panel assembly and form a delta truss, and 6 members that support the solar concentrator on a mounting plate. A principle design requirement was that the assembled concentrator have adequate stiffness so that the fundamental frequency is greater than 1.0 Hz. However, the preliminary design study did not take into consideration potential structural component failures or the replacement of components that degraded or failed. Component structural failures during long-term missions can adversely affect operational conditions, stability and control, and astronaut safety during the repair process.

In the current investigation, finite-element structural analyses of three concepts for a solar concentrator were conducted. The mode shapes were animated to evaluate the relative vibration amplitudes of the components, and the strain energy was computed and used to analyze the results. As a part of the investigation, numerous failure scenarios were postulated and the resulting structural performance was assessed. Those failure conditions that resulted in degraded structural performance were further examined to identify changes and/or alternative structural concepts that would improve the initial structural design of the solar concentrator panel assembly and the support truss.

The analysis results indicate that the fundamental frequency of the baseline system is above the design requirement of 1.0 Hz. The mode shapes for the lowest frequencies are similar to those of a cantilever beam with an attached tip mass. Component failures of the latches that hold the panels together did not significantly degrade the structural performance; however, component failures of the delta truss and support truss reduced the fundamental frequency below the 1.0-Hz limit. Two alternate concepts that replaced the delta truss with a rear-mounted tetrahedral truss were developed and evaluated. One concept incorporated a ring truss, and the other concept incorporated a full truss. Each of these alternate concepts added three additional members to the support truss. The analysis results demonstrate that supporting a shallow interconnected panel system by

a truss is significantly more structurally efficient than interconnecting the panels and supporting them at three points by three tubular beam members. The results also indicate that, based on the mass and structural stiffness of the components used in the analysis model, a full truss support is as structurally efficient as a perimeter truss supplemented by interconnected (latched) panels. Because of the redundancy in the panel latch and the truss-to-panel-attachment mechanism, the full truss may also be easier to design, fabricate, and assemble than the truss and panel latches. Although the proposed undamaged solar dynamic concentrator system is adequate to meet the design requirements, the results of the current investigation indicate that significant improvements in stiffness can be obtained under normal conditions, especially under conditions of structural component failure, by incorporating a support truss for the panels.

NASA Langley Research Center
Hampton, VA 23681-0001
September 13, 1993

References

1. Houck, O. K.; and Heath, A. R., Jr.: *Characteristics of Solar Concentrators as Applied to Space Power Systems*. NASA TM X-54627, 1963.
2. Corrigan, Robert D.; and Ehresman, Derik T.: Solar Concentrator Advanced Development Project. IECEC '87: *Proceedings of the Twenty-Second Intersociety Energy Conversion Engineering Conference, Volume 1*, American Inst. of Aeronautics and Astronautics, 1987, pp. 156-161.
3. Kessler, D. J.: Orbital Debris Issues. *Adv. Space Res.*, vol. 5, no. 2, 1985, pp. 3-10.
4. Secunde, Richard R.; Labus, Thomas L.; and Lovely, Ronald C.: *Solar Dynamic Power Module Design*. NASA TM-102055, 1989.
5. Knasel, Don; and Ehresman, Derik: *Solar Concentrator Advanced Development Program Final Report*. NASA CR-185173, 1989.
6. Collins, Timothy J.; and Fichter, W. B.: *Support Trusses for Large Precision Segmented Reflectors: Preliminary Design and Analysis*. NASA TM-101560, 1989.
7. Heard, Walter L., Jr.; Lake, Mark S.; Bush, Harold G.; Jensen, J. Kermit; Phelps, James E.; and Wallsom, Richard E.: *Extravehicular Activity Compatibility Evaluation of Developmental Hardware for Assembly and Repair of Precision Reflectors*. NASA TP-3246, 1992.
8. Whetstone, W. D.: EISI-EAL Engineering Analysis Language Interim Release, *EAL/325 User Instructions, Version 325.05*. Engineering Information Systems, Inc., Jan. 1990.

Table 1. Structural Mass of Concentrator Components

Component	Number required	Mass per unit, lb	Total component mass, lb
Concept A			
Panel frame	19	33.5	636.5
Reflective facets	456	2.0	912.0
Panel latch	60	4.2	252.0
Delta truss member	3	22.5	67.5
Front support member	2	13.7	27.4
Middle support member	2	20.0	40.0
Rear support member	2	20.0	40.0
			<u>1975.4</u>
Concept B			
Panel frame	19	33.5	636.5
Reflective facets	456	2.0	912.0
Panel latch	60	4.2	252.0
Truss members	132	1.7	224.4
Nodes	42	4.4	184.8
Panel attachments	24	1.3	31.2
Front support member	2	13.7	27.4
Middle support member	2	20.0	40.0
Rear support member	2	20.0	40.0
Additional support members	3	20.0	60.0
			<u>2408.3</u>
Concept C			
Panel frame	19	33.5	636.5
Reflective facets	456	2.0	912.0
Truss members	162	1.7	275.4
Nodes	46	4.4	202.4
Panel attachments	38	1.3	49.4
Front support member	2	13.7	27.4
Middle support member	2	20.0	40.0
Rear support member	2	20.0	40.0
Additional support members	3	20.0	60.0
			<u>2243.1</u>

Table 2. Concentrator Component Structural Properties

Hexagonal panel frame member:

Area, in^2	0.341
Major axis moment of inertia, I_1 , in^4	0.520
Minor axis moment of inertia, I_2 , in^4	0.056
Extensional modulus, E , psi	23.6×10^6
Shear modulus, G , psi	2.6×10^6

Delta and core truss members:

Area, in^2	0.418
Moment of inertia, I , in^4	0.456
Extensional modulus, E , psi	23.6×10^6
Shear modulus, G , psi	2.36×10^6

Panel latch:

Axial stiffness, EA , lb	1.0×10^6
Major axis bending stiffness, EI_1 , lb-in^2	2.6×10^6
Minor axis bending stiffness, EI_2 , lb-in^2	2.5×10^6

Support truss members for concepts B and C:

Area, in^2	0.1250
Moment of inertia, I , in^4	0.0196
Extensional modulus, E , psi	23.6×10^6
Shear modulus, G , psi	2.36×10^6

Panel attachment device for concepts B and C:

Axial stiffness, EA , lb	1.9×10^6
Bending stiffness, EI , lb-in^2	1.26×10^5
Torsional stiffness, GJ , lb-in^2	3.2×10^3

Table 3. Effect of Simulated Failures on Frequencies of Concept A

Mode	Frequency, Hz						
	No failures	Component failure simulated					
		Side delta	Rear delta	Front support	Middle support	Rear support	Latch (worst case) ¹
1	1.64	0.60	0.56	0.14	0.12	0.12	1.47
2	1.97	1.65	1.96	1.64	1.83	1.88	1.70
3	2.15	2.07	2.12	2.09	2.12	2.13	1.98
4	2.30	2.21	2.19	2.25	2.29	2.29	2.15

¹Lowest frequency obtained for any simulated latch failure.

Table 4. Effect of Simulated Failures on Frequencies of Concept B

Mode	Frequency, Hz			
	No failures	Support member removed		
		Front	Middle	Rear
1	1.64	1.48	1.12	1.06
2	2.01	1.81	1.93	1.83
3	3.28	3.13	3.28	3.28

Table 5. Frequencies for First Four Modes of Concepts A, B, and C

Mode	Frequency, Hz		
	Concept A (Mass = 1975.4 lb)	Concept B (Mass = 2428.3 lb)	Concept C (Mass = 2243.1 lb)
1	1.64	1.64	1.17
2	1.97	2.01	2.09
3	2.15	3.28	3.08
4	2.30	3.28	3.09

Table 6. Frequencies of Free-Free Panel Assemblies

Mode	Frequency, Hz			
	Panel only (Mass = 1800.5 lb)	Panel assembly, concept A (Mass = 1868.0 lb)	Panel assembly, concept B (Mass = 2240.9 lb)	Panel assembly, concept C (Mass = 2075.7 lb)
1	0.91	2.05	9.01	8.93
2	.91	2.29	9.02	9.07
3	1.90	2.32	10.74	10.49
4	2.06	3.36	11.23	11.08

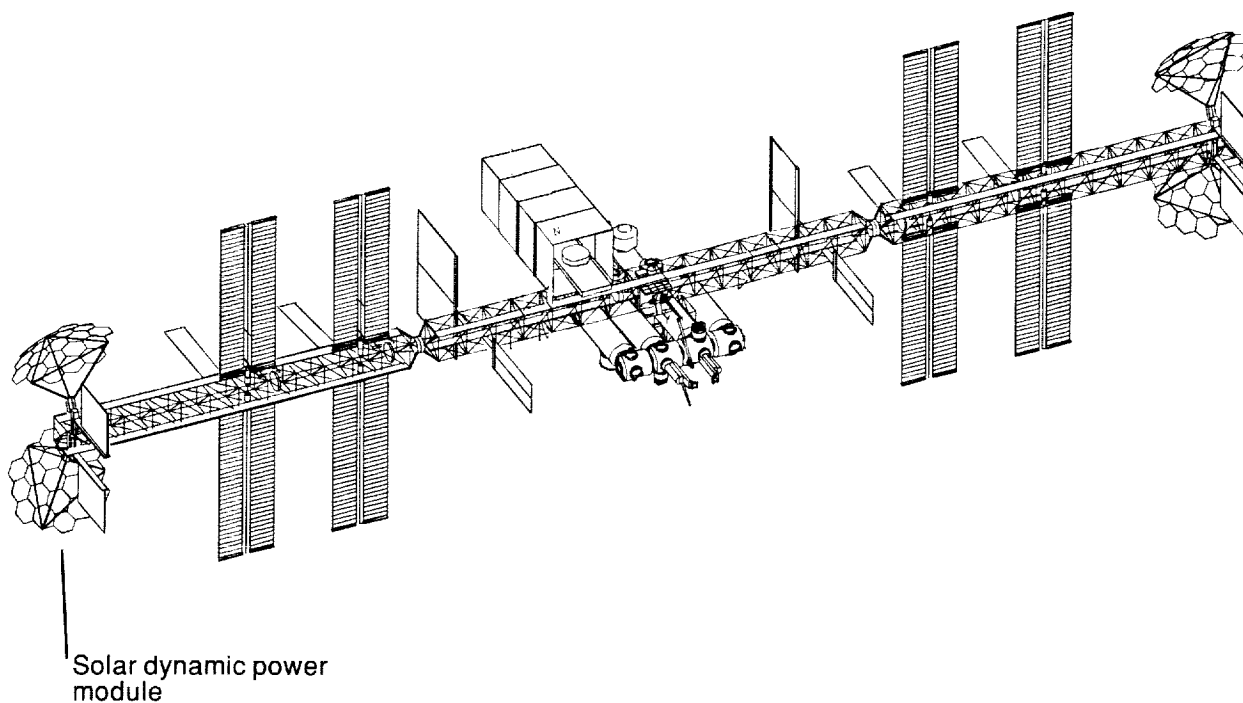


Figure 1. Proposed astronaut-tended space station with four solar dynamic power modules.

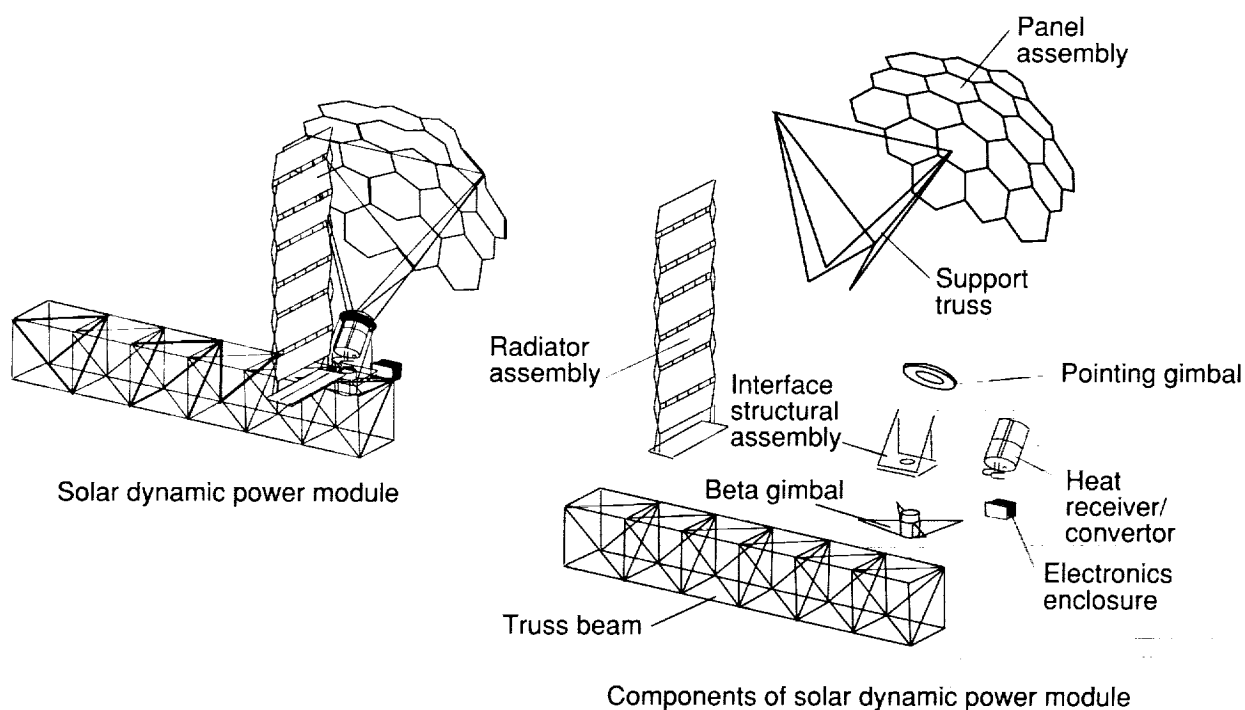
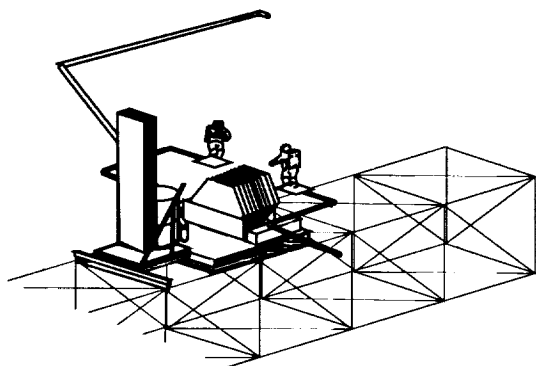
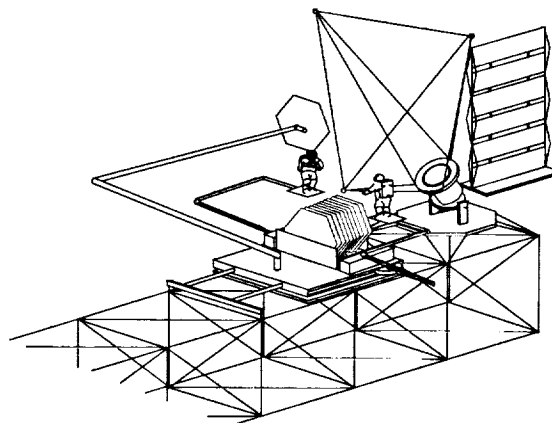


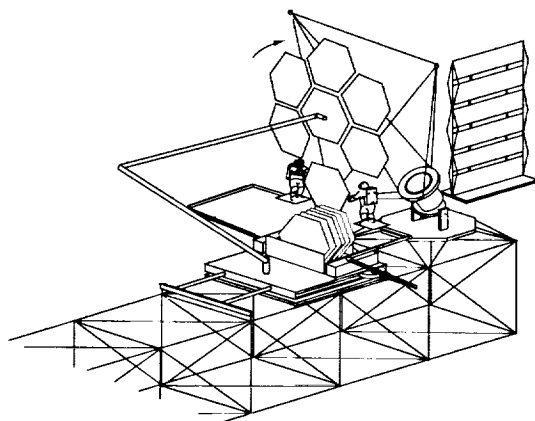
Figure 2. Solar dynamic power module proposed for Space Station *Freedom*.



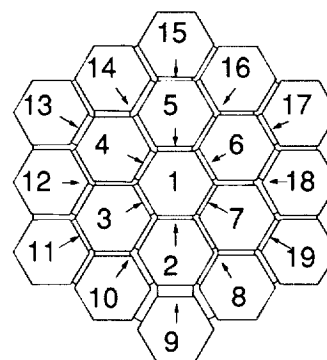
(a) Stored power module.



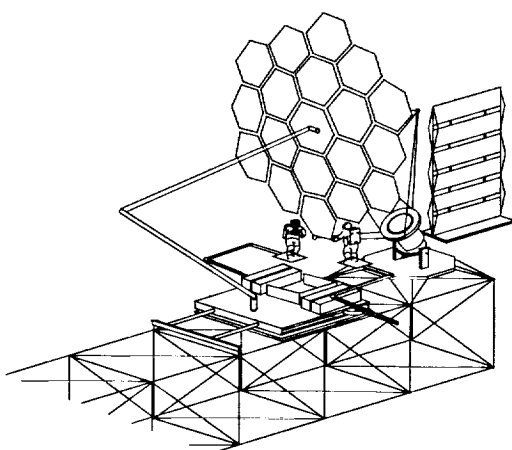
(b) Support truss assembly.



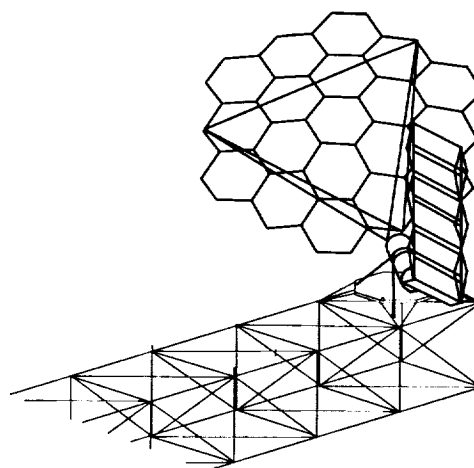
(c) Panel assembly.



(d) Panel insertion sequence.

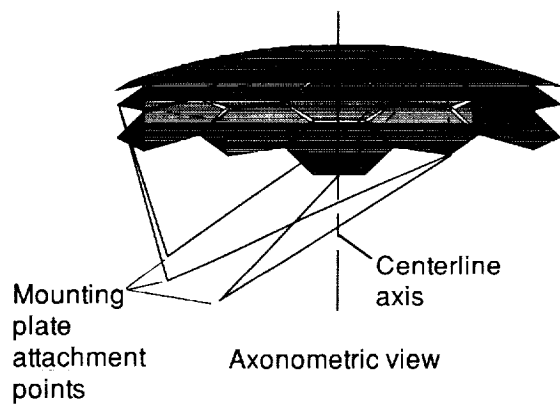


(e) Attachment of panel assembly to support truss.

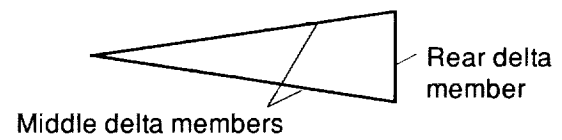


(f) Assembled power module.

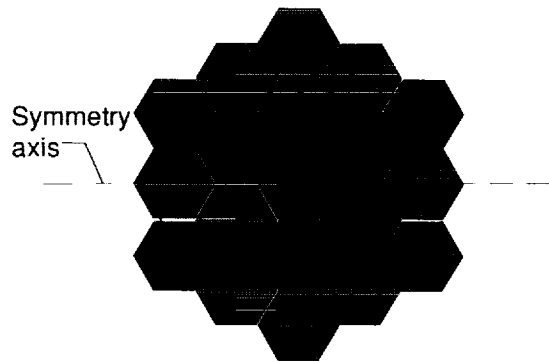
Figure 3. Proposed assembly sequence for solar dynamic power module.



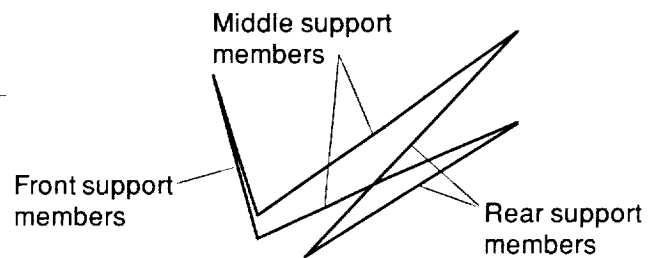
Panel assembly (19 panels)



Delta truss (3 members)

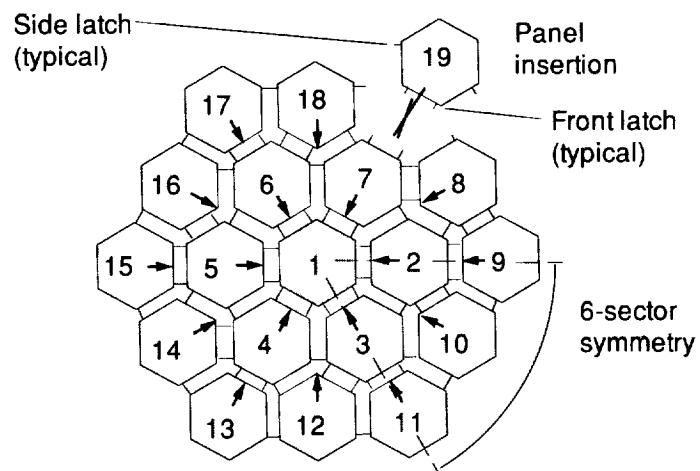


Bottom view

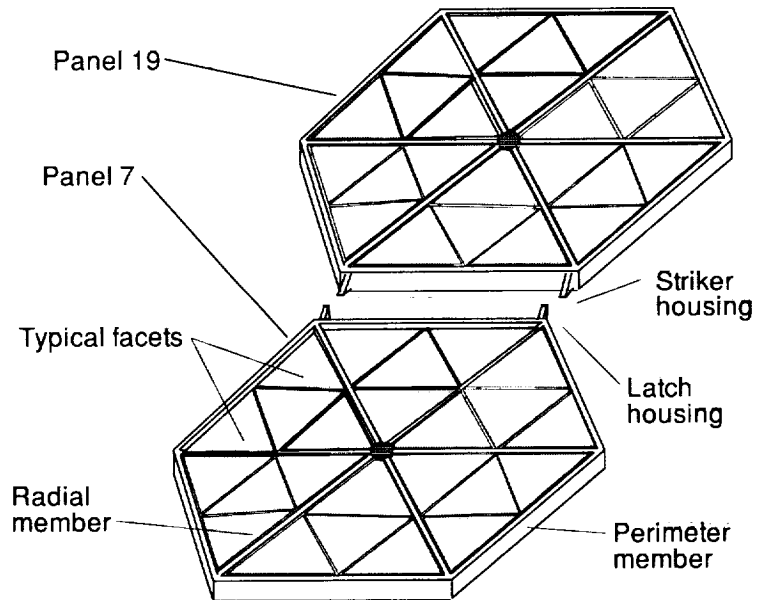


Support truss (6 members)

Figure 4. Panel assembly and support truss for concept A.

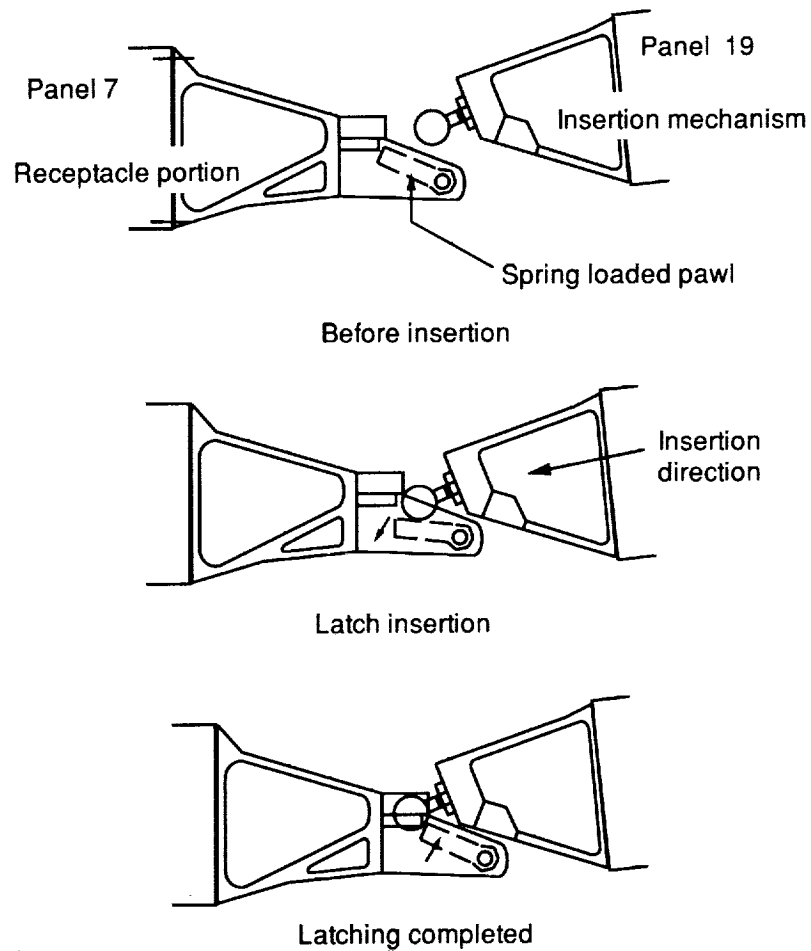


(a) Panel assembly sequence.



(b) Typical hexagonal panel.

Figure 5. Panel assembly and connecting latches for concept A.



(c) Latch operations during assembly.

Figure 5. Concluded.

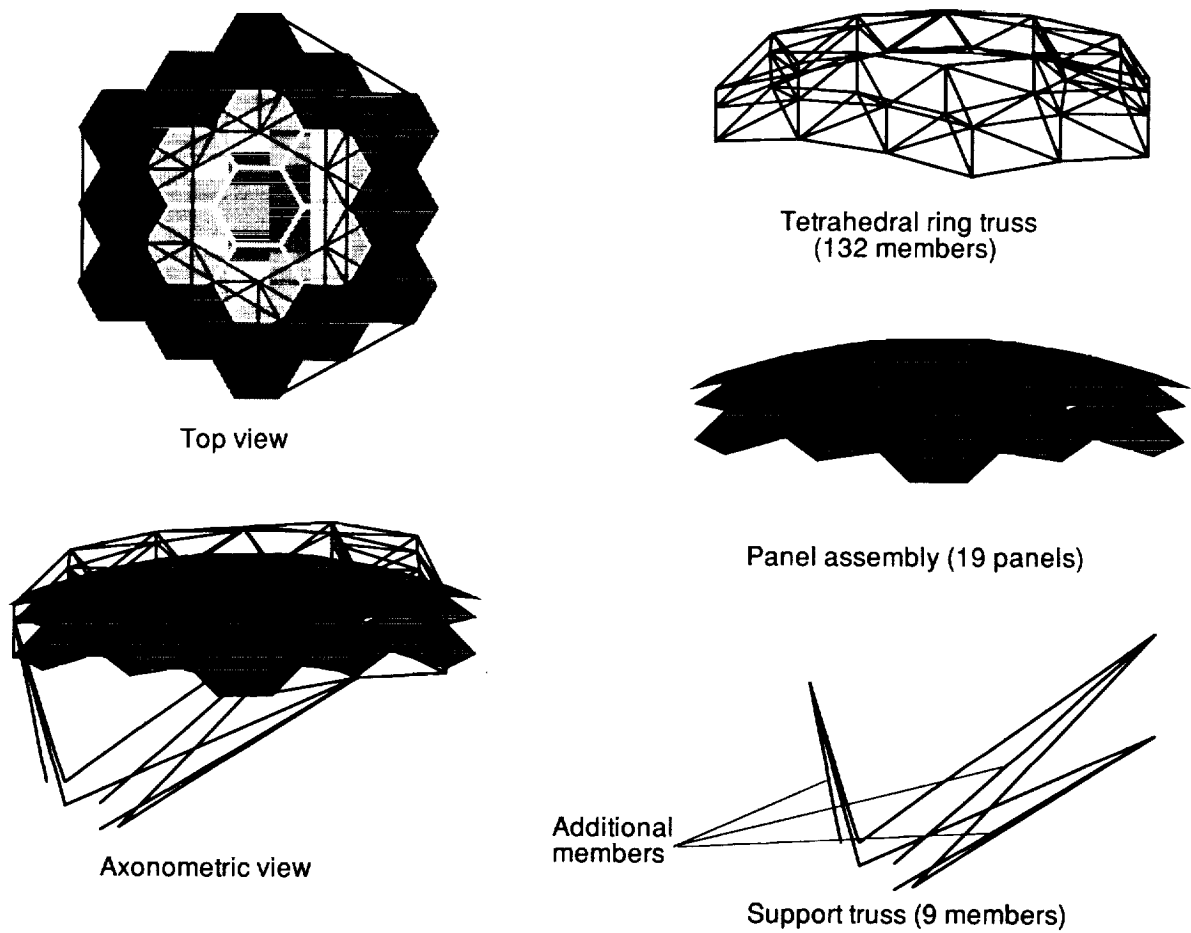


Figure 6. Panel assembly and support truss for concept B. Truss is attached to darker panels.

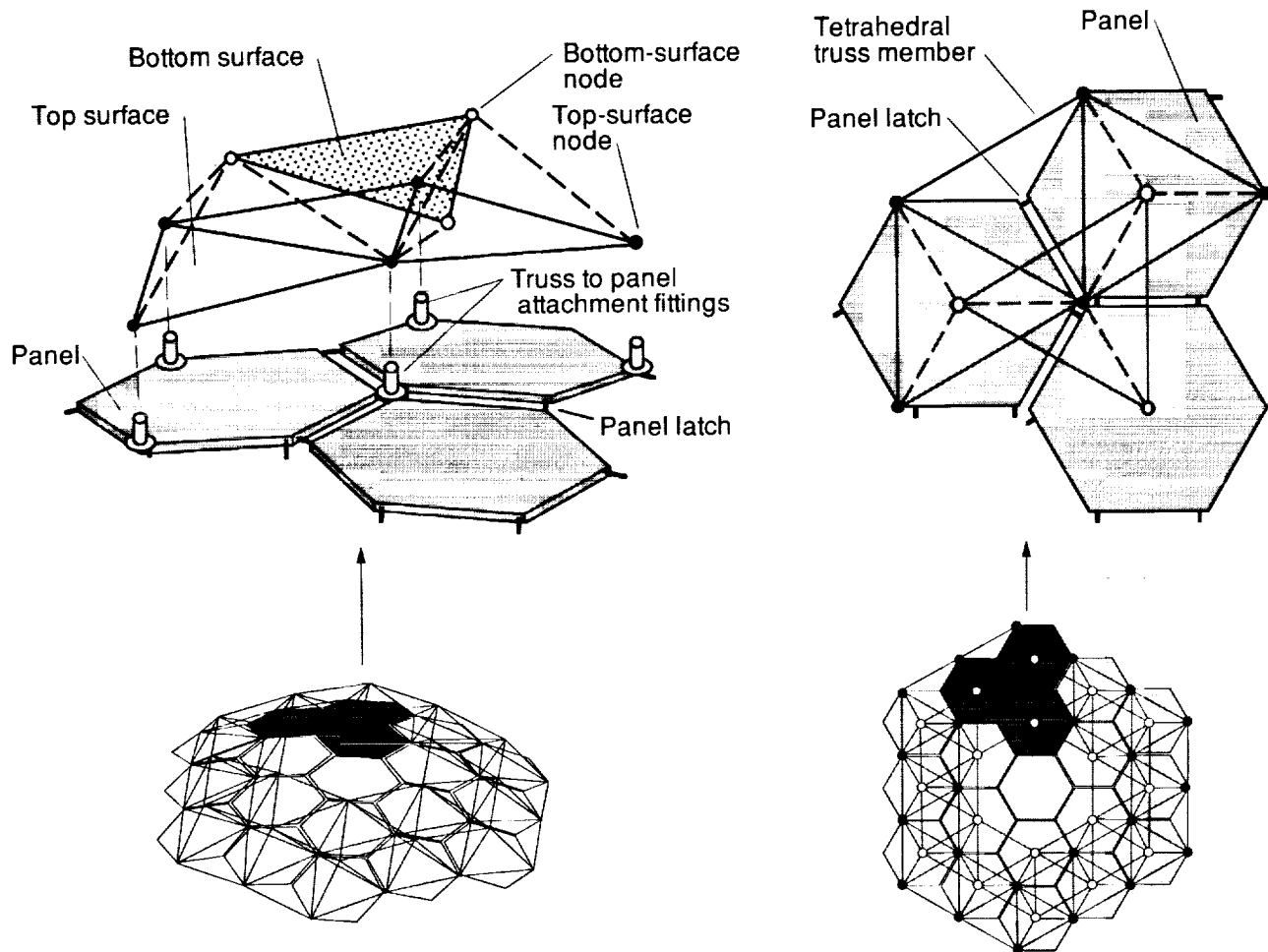


Figure 7. Truss panel attachment fittings for concept B.

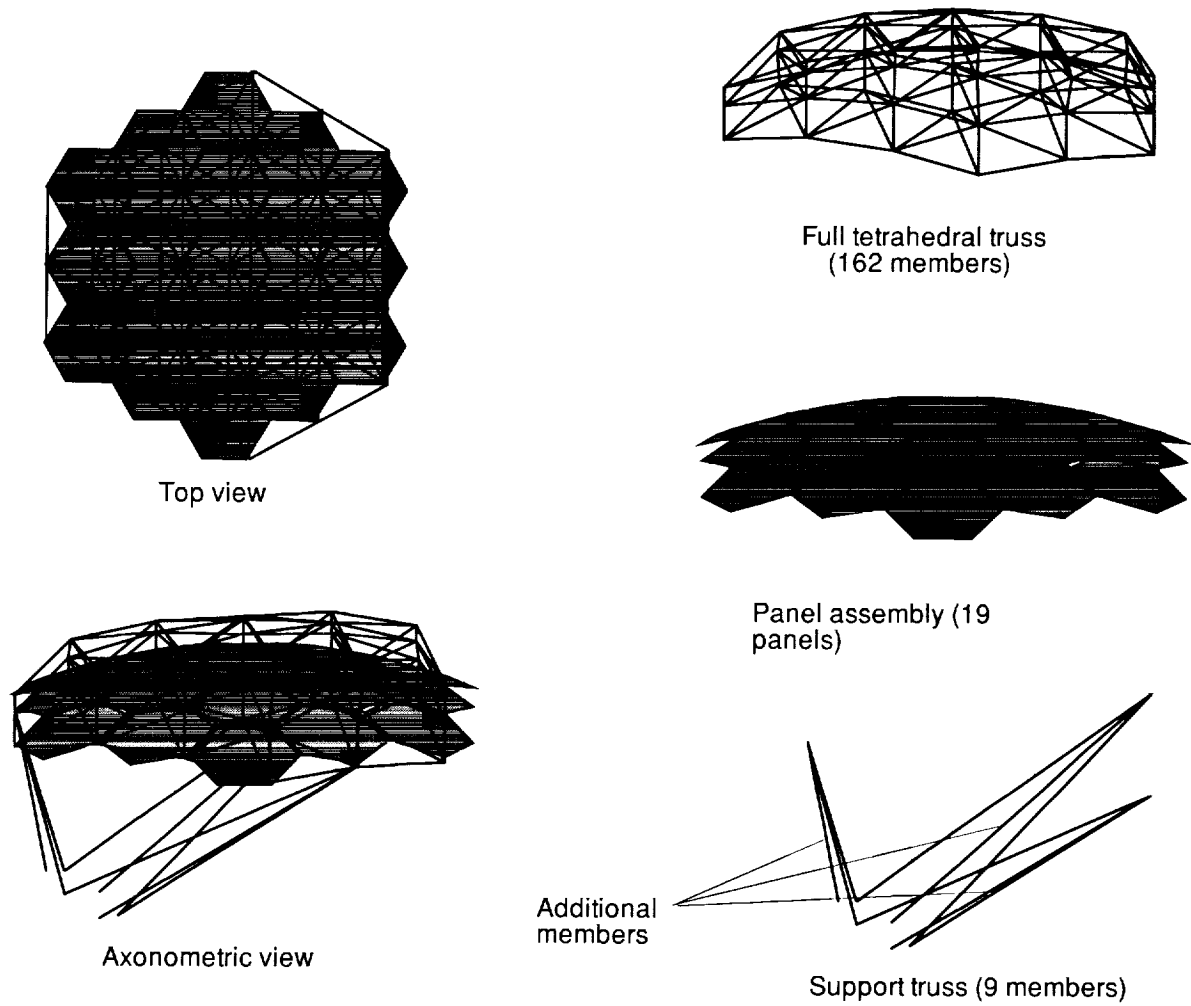


Figure 8. Panel assembly and support truss for concept C.

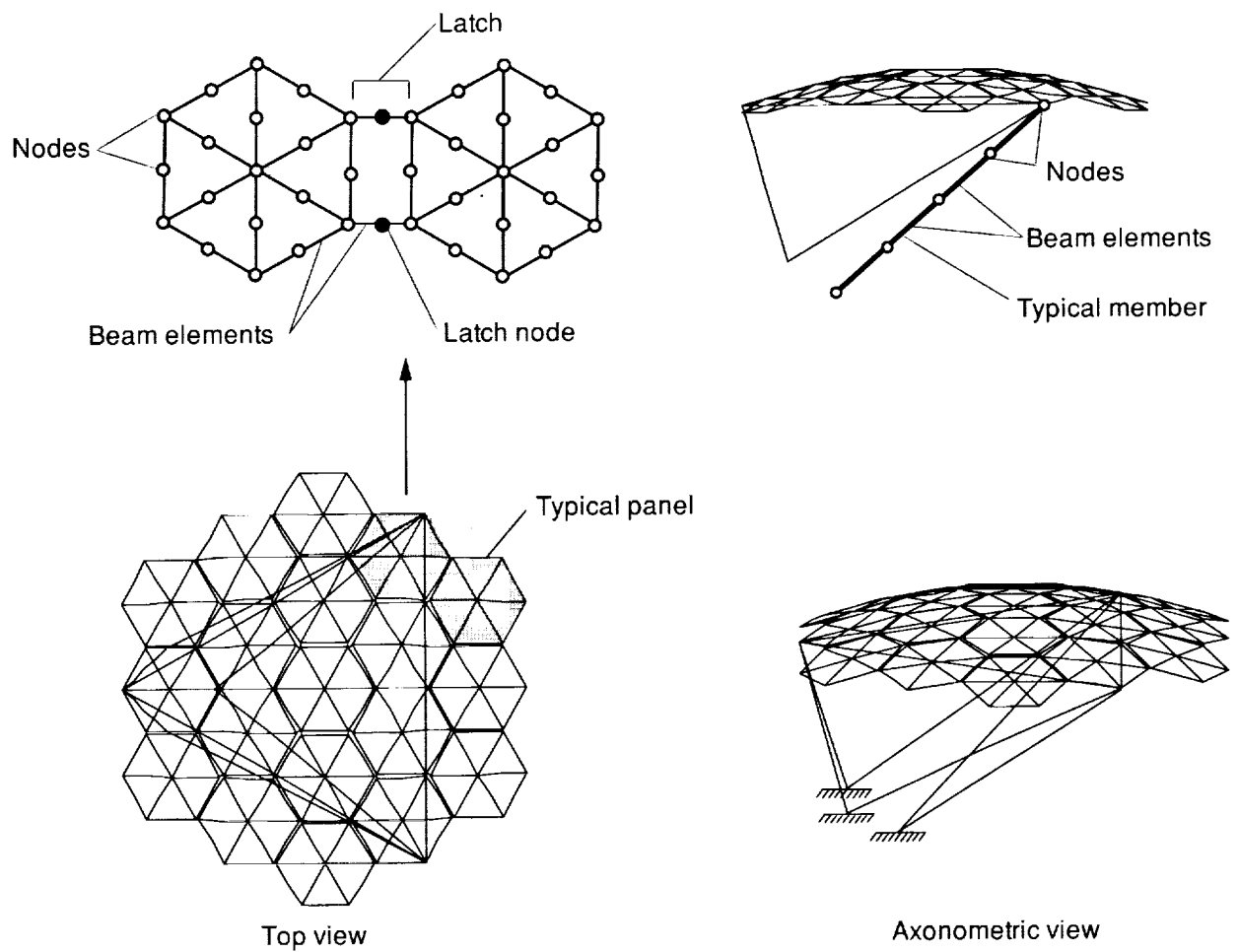


Figure 9. Representation of finite-element model for concept A.

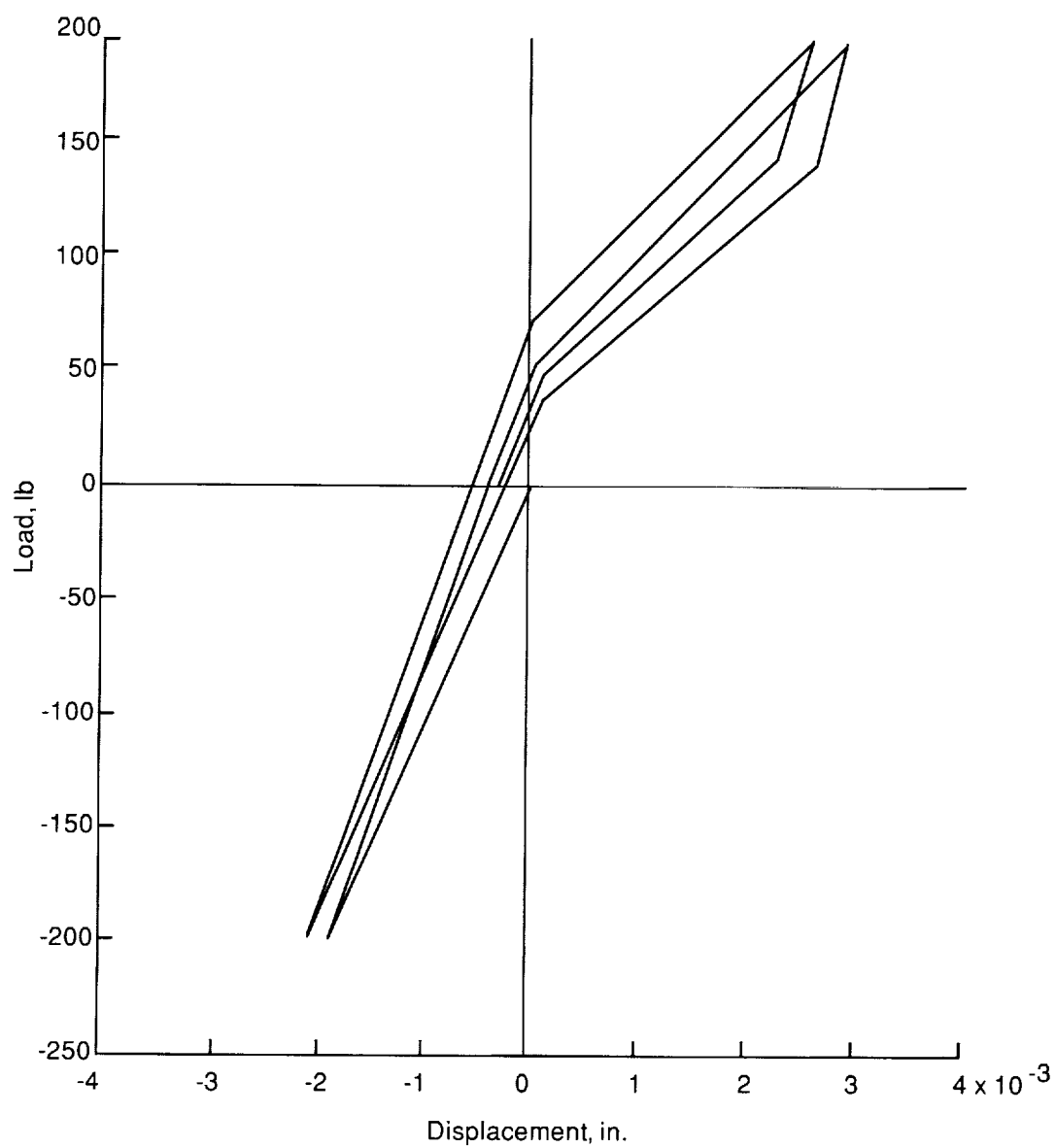
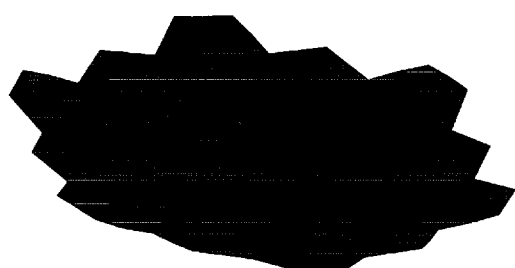


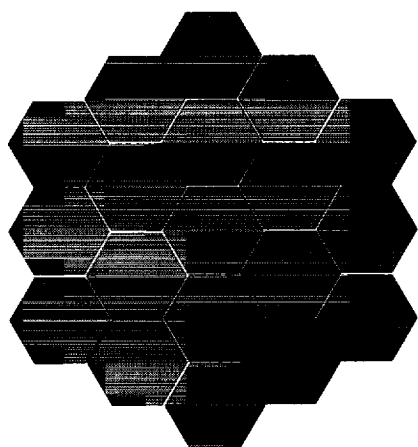
Figure 10. Load-displacement response for representative panel latch.



Perspective view

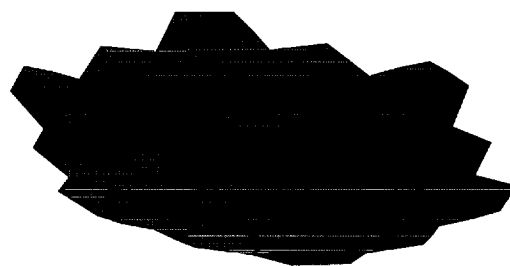


Side view



Bottom view

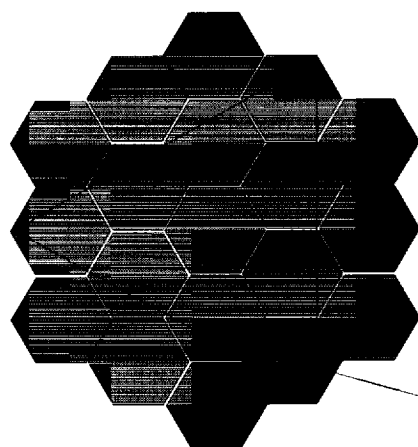
(a) Panel assembly.



Perspective view



Side view



Bottom view

Delta truss

(b) Panel assembly with delta truss.

Figure 11. Free-free panel assemblies analyzed to evaluate influence of delta truss.

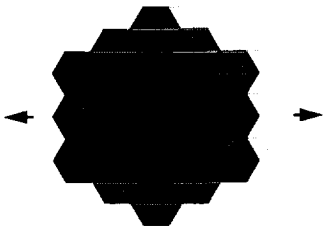
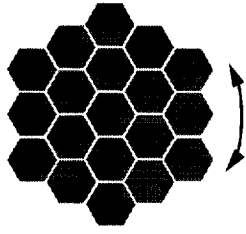
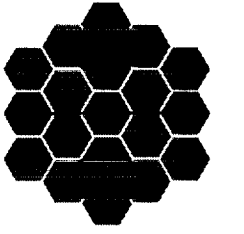
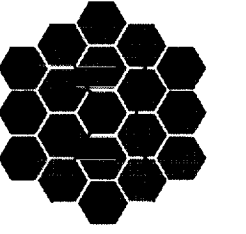
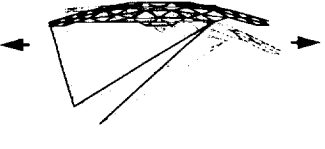
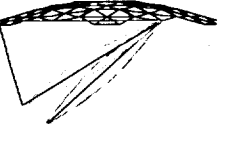

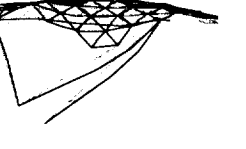
First mode, 1.64 Hz	Second mode, 1.98 Hz	Third mode, 2.15 Hz	Fourth mode, 2.30 Hz
			
			
Distribution of strain energy among components, percent			
<div>Panel assembly 6</div> <div>Support truss 87</div> <div>Delta truss 7</div>	<div>Panel assembly 24</div> <div>Support truss 64</div> <div>Delta truss 12</div>	<div>Panel assembly 72</div> <div>Support truss 19</div> <div>Delta truss 9</div>	<div>Panel assembly 86</div> <div>Support truss 9</div> <div>Delta truss 5</div>

Figure 12. Frequencies and mode shapes for first four modes of concept A. Highlighted components are highest percentage of strain energy.

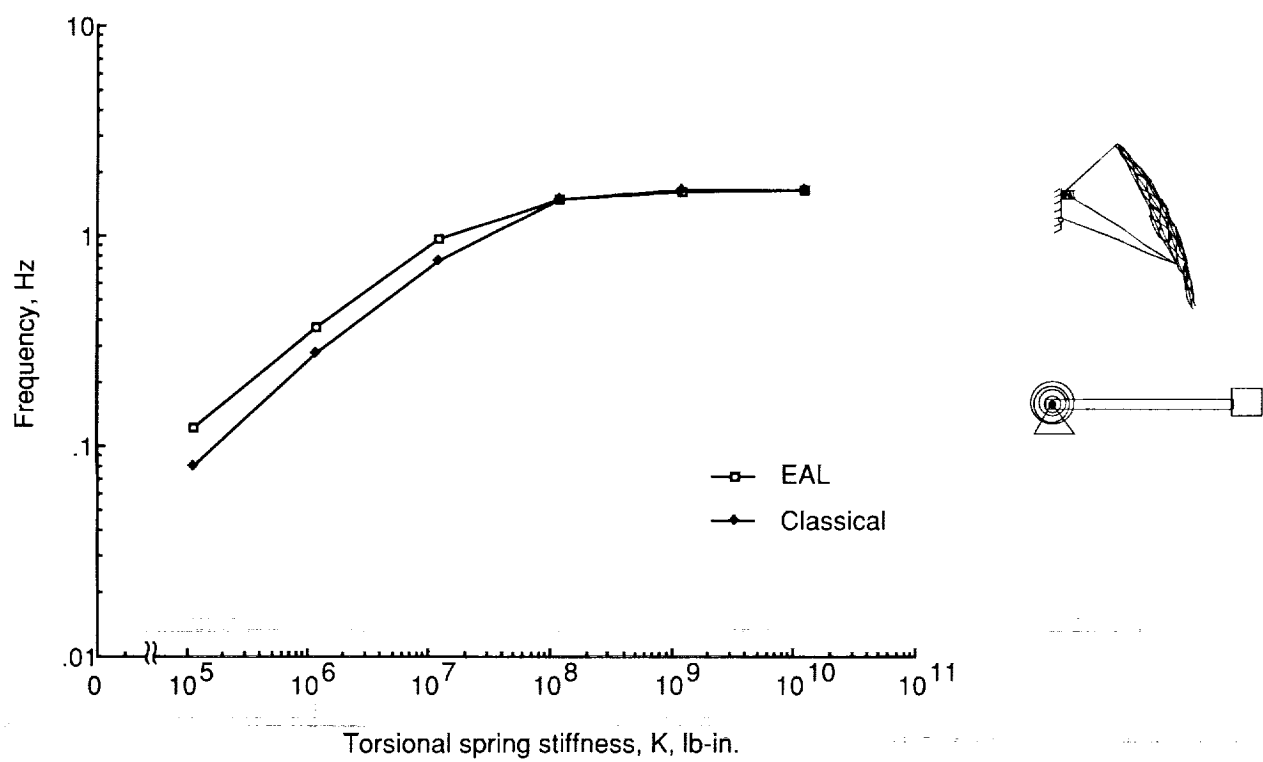
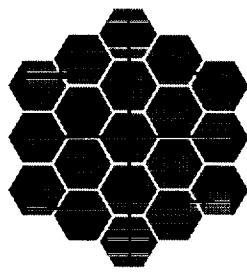
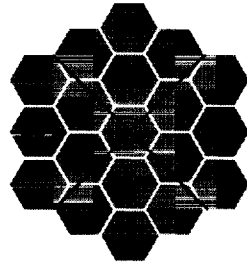


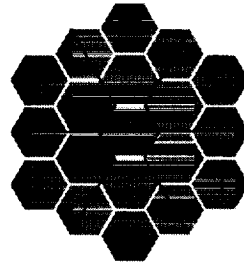
Figure 13. Effect of base support stiffness on fundamental frequency for concept A.



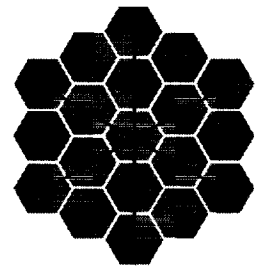
First mode, 0.91 Hz



Second mode, 0.91 Hz

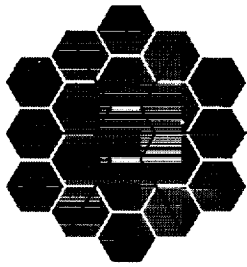


Third mode, 1.90 Hz

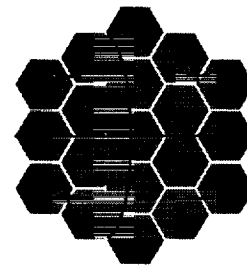


Fourth mode, 2.06 Hz

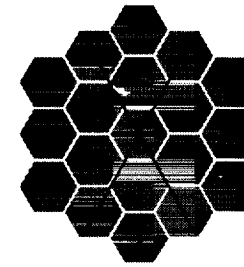
(a) Panel assembly without the delta truss.



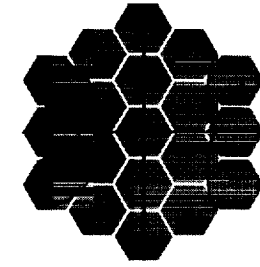
First mode, 2.05 Hz



Second mode, 2.29 Hz



Third mode, 2.32 Hz



Fourth mode, 3.36 Hz

(b) Panel assembly with delta truss.

Figure 14. Free-free response of panel assembly with and without delta truss.

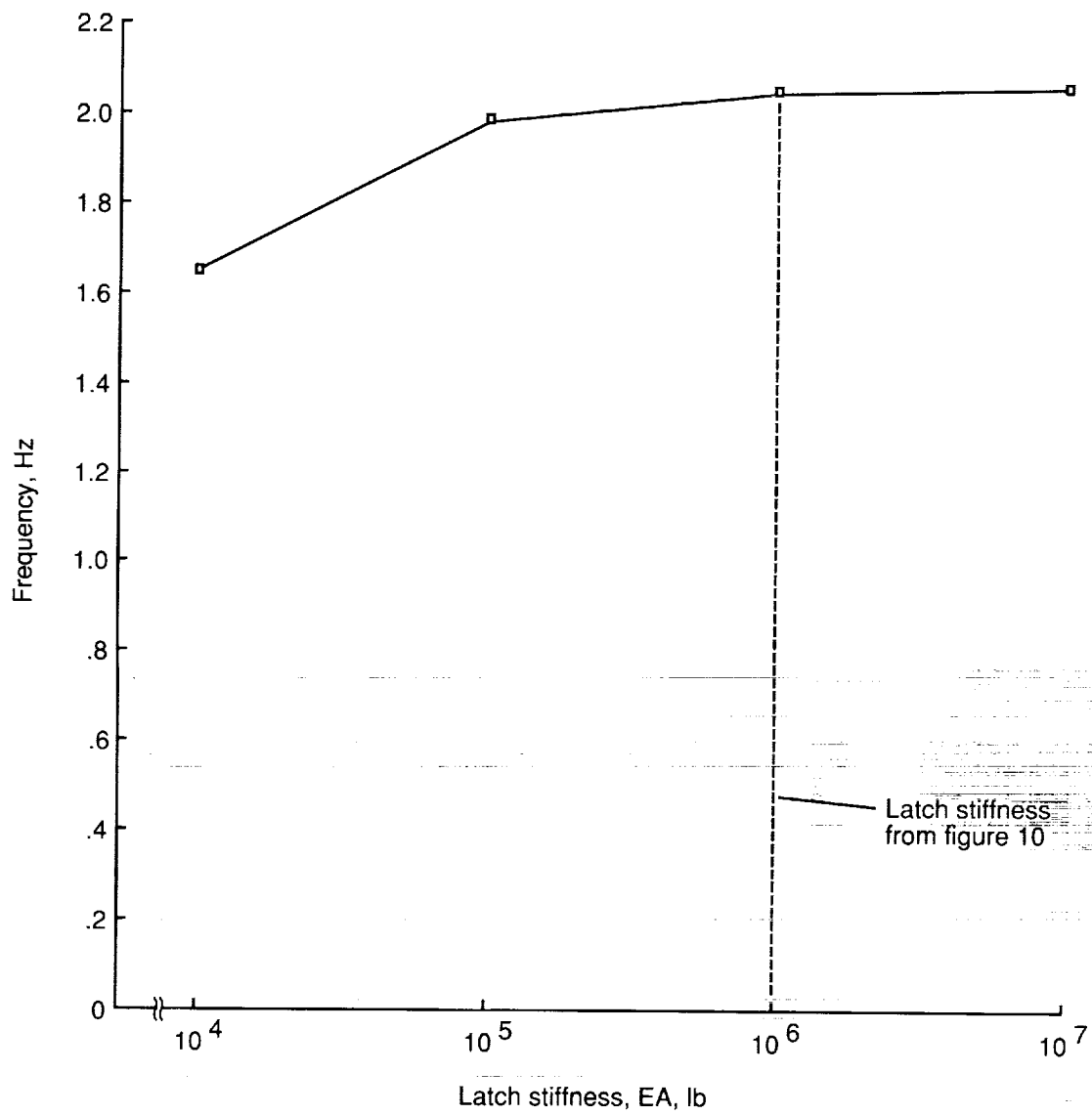


Figure 15. Effect of latch stiffness on free-free vibration frequency of panel assembly and delta truss for concept A.

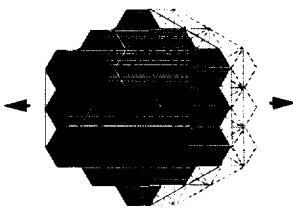
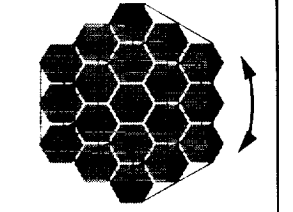
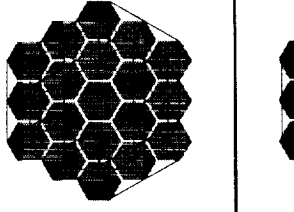
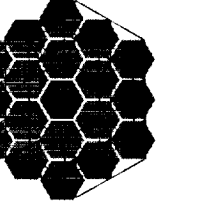
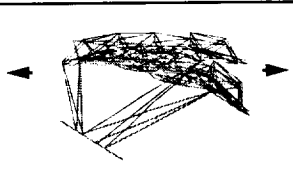
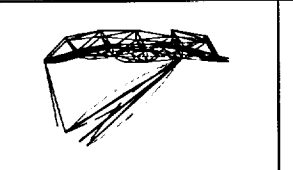
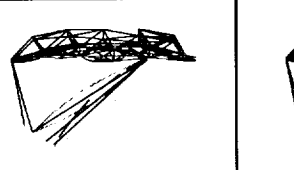

First mode, 1.64 Hz	Second mode, 2.01 Hz	Third mode, 3.28 Hz	Fourth mode, 3.28 Hz
			
			
Distribution of strain energy among components, percent			
Tetrahedral truss 5 Panel assembly 1 <u>Support truss 94</u>	Tetrahedral truss 5 Panel assembly 2 <u>Support truss 93</u>	Tetrahedral truss 12 Panel assembly 6 <u>Support truss 82</u>	Tetrahedral truss 14 Panel assembly 6 <u>Support truss 80</u>

Figure 16. Frequencies and mode shapes for first four modes of concept B. Highlighted components are highest percentage of strain energy.

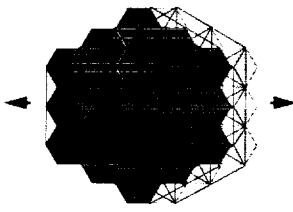
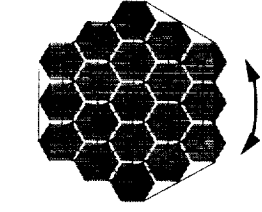
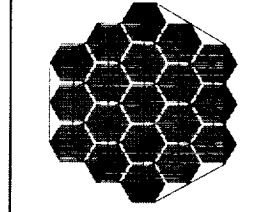
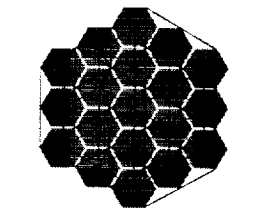
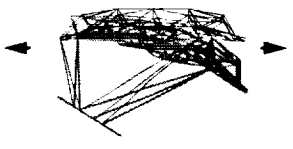



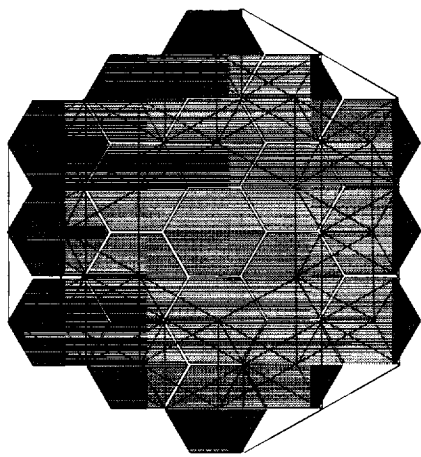
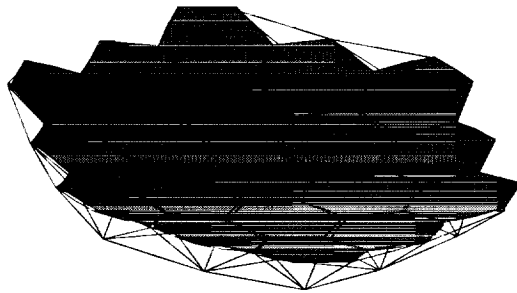
First mode, 1.71 Hz	Second mode, 2.09 Hz	Third mode, 3.08 Hz	Fourth mode, 3.09 Hz
			
			
Distribution of strain energy among components, percent			
Tetrahedral truss 5 Panel assembly 1 Support members 94	Tetrahedral truss 8 Panel assembly 1 Support members 91	Tetrahedral truss 6 Panel assembly 11 Support members 83	Tetrahedral truss 5 Panel assembly 10 Support members 85

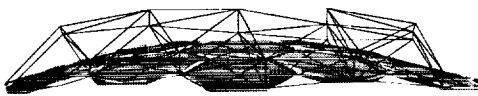
Figure 17. Frequencies and modes for first four modes of concept C. Highlighted components are highest percentage of strain energy.



Top view

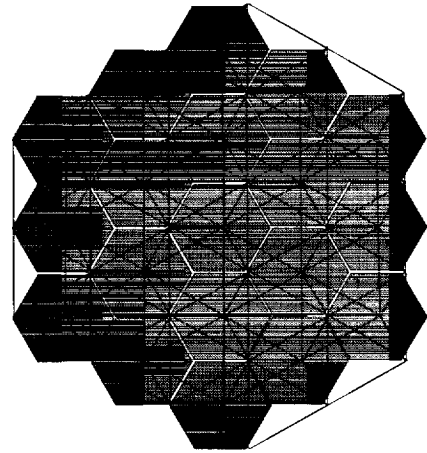


Perspective view

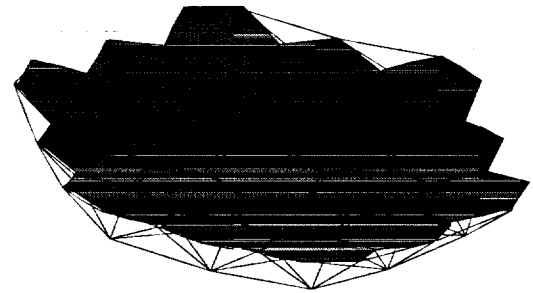


Side view

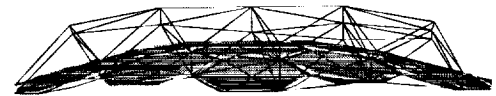
(a) Concept B (132-member truss).



Top view



Perspective view



Side view

(b) Concept C (162-member truss).

Figure 18. Free-free panel assemblies for concepts B and C.

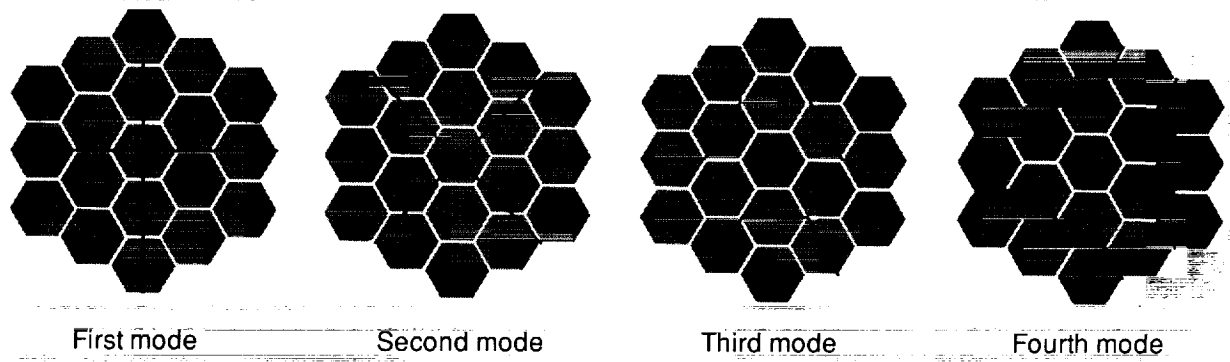


Figure 19. Mode shapes for first four modes of free-free panel assemblies of concepts B and C.

REPORT DOCUMENTATION PAGE			Form Approved OMB No. 0704-0188	
Public reporting burden for this collection of information is estimated to average 1 hour per response, including the time for reviewing instructions, searching existing data sources, gathering and maintaining the data needed, and completing and reviewing the collection of information. Send comments regarding this burden estimate or any other aspect of this collection of information, including suggestions for reducing this burden, to Washington Headquarters Services, Directorate for Information Operations and Reports, 1215 Jefferson Davis Highway, Suite 1204, Arlington, VA 22202-4302, and to the Office of Management and Budget, Paperwork Reduction Project (0704-0188), Washington, DC 20503.				
1. AGENCY USE ONLY (Leave blank)	2. REPORT DATE February 1994	3. REPORT TYPE AND DATES COVERED Technical Paper		
4. TITLE AND SUBTITLE Structural Evaluation of Concepts for a Solar Energy Concentrator for Space Station Advanced Development Program		5. FUNDING NUMBERS WU 506-43-41-02		
6. AUTHOR(S) Winfred S. Kenner and Marvin D. Rhodes				
7. PERFORMING ORGANIZATION NAME(S) AND ADDRESS(ES) NASA Langley Research Center Hampton, VA 23681-0001		8. PERFORMING ORGANIZATION REPORT NUMBER L-17239		
9. SPONSORING/MONITORING AGENCY NAME(S) AND ADDRESS(ES) National Aeronautics and Space Administration Washington, DC 20546-0001		10. SPONSORING/MONITORING AGENCY REPORT NUMBER NASA TP-3375		
11. SUPPLEMENTARY NOTES				
12a. DISTRIBUTION/AVAILABILITY STATEMENT Unclassified-Unlimited Subject Category 18		12b. DISTRIBUTION CODE		
13. ABSTRACT (Maximum 200 words) Solar dynamic power systems have a higher thermodynamic efficiency than conventional photovoltaic systems; therefore, they are attractive for long-term space missions with high electrical power demands. In an investigation conducted in support of a preliminary concept for Space Station <i>Freedom</i> , a novel approach for a solar dynamic power system was developed and a number of the components for the solar concentrator were fabricated for experimental evaluation. The concentrator consists of hexagonal panels comprised of triangular reflective facets which are supported by a truss. In the current investigation, structural analyses of the solar concentrator and the support truss were conducted using finite-element models. As a part of the investigation, a number of potential component failure scenarios were postulated and the resulting structural performance was assessed. The solar concentrator and support truss were found to be adequate to meet a 1.0-Hz structural dynamics design requirement in pristine condition. However, for some of the simulated component failure conditions, the fundamental frequency dropped below the 1.0-Hz design requirement. As a result, two alternative concepts were developed and assessed. One concept incorporated a tetrahedral ring truss support for the hexagonal panels; the second incorporated a full tetrahedral truss support for the panels. The results indicate that significant improvements in stiffness can be obtained by attaching the panels to a tetrahedral truss, and that this concentrator and support truss will meet the 1.0-Hz design requirement with any of the simulated failure conditions.				
14. SUBJECT TERMS Large space structures; Component failure; Dynamic characteristics; Solar dynamic power; Reflectors			15. NUMBER OF PAGES 31	
			16. PRICE CODE A03	
17. SECURITY CLASSIFICATION OF REPORT Unclassified	18. SECURITY CLASSIFICATION OF THIS PAGE Unclassified	19. SECURITY CLASSIFICATION OF ABSTRACT	20. LIMITATION OF ABSTRACT	